

The ^{154}Gd neutron capture cross section measured at the n_TOF facility and its astrophysical implications

M. Mastromarco^{1,2,*}, *A. Mazzone*^{3,4}, *C. Massimi*^{5,6}, *S. Cristallo*^{7,8}, *N. Colonna*³, *O. Aberle*¹, *V. Alcayne*⁹, *S. Amaducci*^{10,11}, *J. Andrzejewski*¹², *L. Audouin*¹³, *V. Babiano-Suarez*¹⁴, *M. Bacak*^{1,15,16}, *M. Barbagallo*^{1,3}, *S. Bennett*², *E. Berthoumieux*¹⁶, *D. Bosnar*¹⁷, *A. S. Brown*¹⁸, *M. Busso*^{7,19}, *M. Caamaño*²⁰, *L. Caballero*¹⁴, *M. Calviani*¹, *F. Calviño*²¹, *D. Cano-Ott*⁹, *A. Casanovas*²¹, *F. Cerutti*¹, *E. Chiaveri*^{2,22,1}, *G. P. Cortés*²¹, *M. A. Cortés-Giraldo*²², *L. Cosentino*¹⁰, *L. A. Damone*^{3,23}, *P. J. Davies*², *M. Diakaki*²⁴, *M. Dietz*²⁵, *C. Domingo-Pardo*¹⁴, *R. Dressler*²⁶, *Q. Ducasse*²⁷, *E. Dupont*¹⁶, *I. Durán*²⁰, *Z. Eleme*²⁸, *B. Fernández-Domínguez*²⁰, *A. Ferrari*¹, *I. Ferro-Gonçalves*²⁹, *P. Finocchiaro*¹⁰, *V. Furman*³⁰, *R. Garg*²⁵, *A. Gawlik*¹², *S. Gilardoni*¹, *K. Göbel*³¹, *E. González-Romero*⁹, *C. Guerrero*²², *F. Gunsing*¹⁶, *S. Heinitz*²⁶, *J. Heyse*³², *D. G. Jenkins*¹⁸, *E. Jericha*¹⁵, *U. Jiri*²⁶, *A. Junghans*³³, *Y. Kadi*¹, *F. Käppeler*³⁴, *A. Kimura*³⁵, *I. Knapová*³⁶, *M. Kokkoris*²⁴, *Y. Kopatch*³⁰, *M. Krtička*³⁶, *D. Kurtulgil*³¹, *I. Ladarescu*¹⁴, *C. Lederer-Woods*²⁵, *J. Lerendegui-Marco*²², *S.-J. Lonsdale*²⁵, *D. Macina*¹, *A. Manna*^{5,6}, *T. Martínez*⁹, *A. Masi*¹, *P. F. Mastinu*³⁷, *E. Mauger*²⁶, *E. Mendoza*⁹, *A. Mengoni*^{38,5}, *V. Michalopoulou*^{1,24}, *P. M. Milazzo*³⁹, *M. A. Millán-Callado*²², *F. Mingrone*¹, *J. Moreno-Soto*¹⁶, *A. Musumarra*^{10,11}, *A. Negret*⁴⁰, *F. Ogállar*⁴¹, *A. Oprea*⁴⁰, *N. Patronis*²⁸, *A. Pavlik*⁴², *J. Perkowski*¹², *C. Petrone*⁴⁰, *L. Piersanti*^{7,8}, *E. Pirovano*²⁷, *I. Porras*⁴¹, *J. Praena*⁴¹, *J. M. Quesada*²², *D. Ramos Doval*¹³, *R. Reifarth*³¹, *D. Rochman*²⁶, *C. Rubbia*¹, *M. Sabaté-Gilarte*^{22,1}, *A. Saxena*⁴³, *P. Schillebeeckx*³², *D. Schumann*²⁶, *A. Sekhar*², *A. G. Smith*², *N. Sosnin*², *P. Sprung*²⁶, *A. Stamatopoulos*²⁴, *G. Tagliente*³, *J. L. Tain*¹⁴, *A. E. Tarifeño-Saldivia*²¹, *L. Tassan-Got*^{1,24,13}, *B. Thomas*³¹, *P. Torres-Sánchez*⁴¹, *A. Tsinganis*¹, *S. Urlass*^{1,33}, *S. Valenta*³⁶, *G. Vannini*^{5,6}, *V. Variale*³, *P. Vaz*²⁹, *A. Ventura*⁵, *D. Vescovi*^{7,44}, *V. Vlachoudis*¹, *R. Vlastou*²⁴, *A. Wallner*⁴⁵, *P. J. Woods*²⁵, *T. J. Wright*², and *P. Žugec*¹⁷

¹European Organization for Nuclear Research (CERN), Switzerland

²University of Manchester, United Kingdom

³Istituto Nazionale di Fisica Nucleare, Bari, Italy

⁴Consiglio Nazionale delle Ricerche, Bari, Italy

⁵Istituto Nazionale di Fisica Nucleare, Sezione di Bologna, Italy

⁶Dipartimento di Fisica e Astronomia, Università di Bologna, Italy

⁷Istituto Nazionale di Fisica Nucleare, Perugia, Italy

⁸Istituto Nazionale di Astrofisica - Osservatorio Astronomico d'Abruzzo, Italy

⁹Centro de Investigaciones Energéticas Medioambientales y Tecnológicas (CIEMAT), Spain

¹⁰INFN Laboratori Nazionali del Sud, Catania, Italy

¹¹Dipartimento di Fisica e Astronomia, Università di Catania, Italy

¹²University of Lodz, Poland

¹³IPN, CNRS-IN2P3, Univ. Paris-Sud, Université Paris-Saclay, F-91406 Orsay Cedex, France

¹⁴Instituto de Física Corpuscular, CSIC - Universidad de Valencia, Spain

¹⁵Technische Universität Wien, Austria

¹⁶CEA Saclay, Irfu, Université Paris-Saclay, Gif-sur-Yvette, France

¹⁷Department of Physics, Faculty of Science, University of Zagreb, Croatia

¹⁸University of York, United Kingdom

¹⁹Dipartimento di Fisica e Geologia, Università di Perugia, Italy

²⁰University of Santiago de Compostela, Spain

²¹Universitat Politècnica de Catalunya, Spain

²²Universidad de Sevilla, Spain

²³Dipartimento di Fisica, Università degli Studi di Bari, Italy

²⁴National Technical University of Athens, Greece

²⁵School of Physics and Astronomy, University of Edinburgh, United Kingdom

²⁶Paul Scherrer Institut (PSI), Villigen, Switzerland

²⁷Physikalisch-Technische Bundesanstalt (PTB), Bundesallee 100, 38116 Braunschweig, Germany

²⁸University of Ioannina, Greece

²⁹Instituto Superior Técnico, Lisbon, Portugal

³⁰Joint Institute for Nuclear Research (JINR), Dubna, Russia

³¹Goethe University Frankfurt, Germany

³²European Commission, Joint Research Centre, Geel, Retieseweg 111, B-2440 Geel, Belgium

³³Helmholtz-Zentrum Dresden-Rossendorf, Germany

³⁴Karlsruhe Institute of Technology, Campus North, IKP, 76021 Karlsruhe, Germany

³⁵Japan Atomic Energy Agency (JAEA), Tokai-mura, Japan

³⁶Charles University, Prague, Czech Republic

³⁷Istituto Nazionale di Fisica Nucleare, Sezione di Legnaro, Italy

³⁸Agenzia nazionale per le nuove tecnologie, l'energia e lo sviluppo economico sostenibile (ENEA), Bologna, Italy

³⁹Istituto Nazionale di Fisica Nucleare, Trieste, Italy

⁴⁰Horia Hulubei National Institute of Physics and Nuclear Engineering (IFIN-HH), Bucharest

⁴¹University of Granada, Spain

⁴²University of Vienna, Faculty of Physics, Vienna, Austria

⁴³Bhabha Atomic Research Centre (BARC), India

⁴⁴Gran Sasso Science Institute (GSSI), L'Aquila, Italy

⁴⁵Australian National University, Canberra, Australia

Abstract. The (n, γ) cross sections of the gadolinium isotopes play an important role in the study of the stellar nucleosynthesis. In particular, among the isotopes heavier than Fe, ^{154}Gd together with ^{152}Gd have the peculiarity to be mainly produced by the slow capture process, the so-called s-process, since they are shielded against the β -decay chains from the r-process region by their stable samarium isobars. Such a quasi pure s-process origin makes them crucial for testing the robustness of stellar models in galactic chemical evolution (GCE). According to recent models, the ^{154}Gd and ^{152}Gd abundances are expected to be 15-20% lower than the reference un-branched s-process ^{150}Sm isotope. The close correlation between stellar abundances and neutron capture cross sections prompted for an accurate measurement of ^{154}Gd cross section in order to reduce the uncertainty attributable to nuclear physics input and eventually rule out one of the possible causes of present discrepancies between observation and model predictions. To this end, the neutron capture cross section of ^{154}Gd was measured in a wide neutron energy range (from thermal up to some keV) with high resolution in the first experimental area of the neutron time-of-flight facility n_TOF (EAR1) at CERN. In this contribution, after a brief description of the motivation and of the experimental setup used in the measurement, the preliminary results of the ^{154}Gd neutron capture reaction as well as their astrophysical implications are presented.

1 Introduction

Neutron-induced reactions and β -decays are the main nuclear processes involved in the formation of elements heavier than iron. In particular, two main processes have been identified so far: the slow neutron-capture process (s-process) and the rapid one (r-process). The latter is responsible for the production of approximately half of the atomic nuclei heavier than iron and it is thought to take place in neutron stars mergers and Supernovae. The remaining half is synthesized via the s-process. Depending on the initial mass of the star, different regimes can be considered: the so called weak s-process component in Massive stars and the Main s-process component in the Asymptotic Giant Branch (AGB) phase of low-to-intermediate mass stars [1].

In this context, the ${}^n\text{Gd}(n, \gamma)^{n+1}\text{Gd}$ cross sections play an important role in the detailed study of the s-process nucleosynthesis. In particular, the even isotopes $^{152,154}\text{Gd}$, unlike most of the isotopes heavier than iron, are mainly produced via the s-process because they are shielded against the β -decay chains from the r-process region by the stable samarium isobars¹. In Figure 1 we show the s-process path in the Sm-Eu-Gd-Tb region.

Because of their quasi pure s-process nature, neutron capture reactions on even gadolinium isotopes ($^{152,154}\text{Gd}$) are essential ingredients to test the reliability of Galactic Chemical Evolution (CGE) models [2]. However, as shown in Figure 2, CGE calculations yield abundances for these isotopes up to 20% below the reference un-branched s-process isotope ^{150}Sm ([3, 4]). A possible explanation

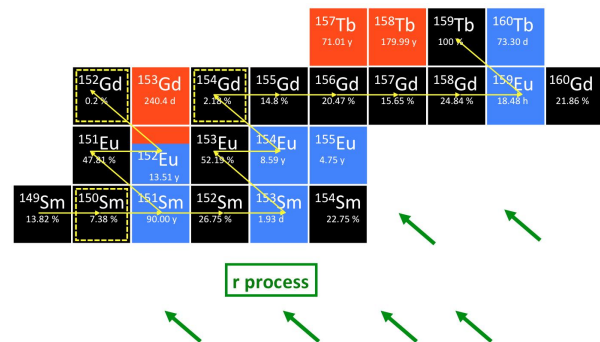


Figure 1. The Sm-Eu-Gd-Tb region: we plot stable isotopes in black (natural abundances are reported), β^- emitters in blue and β^+ in red (together with their half-lives). S-only isotopes are marked by yellow double-framed quadrangles.

for this disagreement was sought in the neutron-capture cross section of $^{152,154}\text{Gd}$ which strongly affects the isotopic abundances.

To date, from an experimental point of view, the status of the gadolinium cross sections is still not completely clear. In particular, given the low natural abundance of the two s-only isotopes ^{152}Gd and ^{154}Gd , large uncertainties in their cross sections are present because of isotopic impurities corrections. This situation prompted the n_TOF Collaboration to perform a new measurement of the capture cross section for the ^{154}Gd isotope from thermal to 1 MeV neutron energy at the CERN neutron time-of-flight facility, n_TOF. In this work, preliminary results and related astrophysical implications are reported.

*e-mail: mario.mastromarco@cern.ch

¹The possible contribution from the p-process is currently matter of debate.

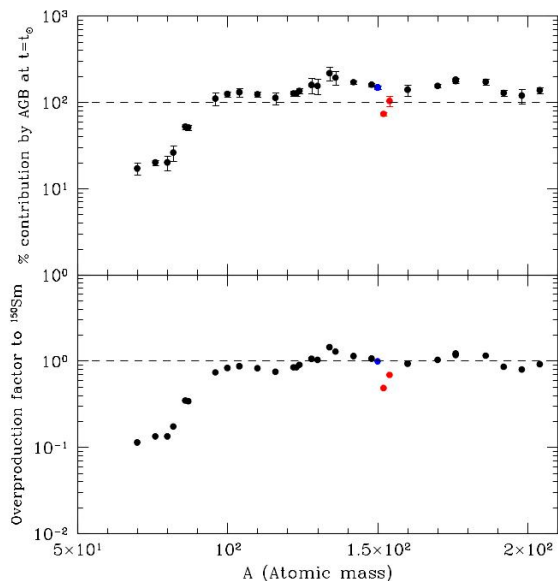


Figure 2. Upper panel: percentage s-only isotopic abundances at the epoch of the solar system formation (adapted from [4]). Solar abundance errors are taken from [5]; 100% contribution means that an isotope is entirely synthesized. Lower panel: overproduction factors normalized to ^{150}Sm . The two red points correspond to the $^{152,154}\text{Gd}$ isotopes.

2 The experimental setup

2.1 The n_TOF facility

At the n_TOF facility neutrons are produced by spallation processes induced by 20 GeV/c protons from the CERN Proton Synchrotron (PS), impinging on a massive cylindrical lead target, 40 cm in length and 60 cm in diameter. Fast neutrons are initially moderated by a first layer of 1 cm of demineralized water plus a second layer of 4 cm of borated water, resulting in a neutron flux spanning from thermal energy up to the GeV region (see [6] for more details). Because of the better resolving power (relative resolution $\approx 5.4 \times 10^{-4}$ at 1 keV), the $^{154}\text{Gd}(n, \gamma)$ measurement was carried out in the first experimental area (EAR1), located at 185 m distance from the spallation target.

2.2 Detection system and samples

Four deuterated benzene (C_6D_6) liquid scintillation detectors have been used to detect γ -rays emitted after a neutron capture event (see Figure 3). These detectors, characterized by a very low neutron sensitivity [7], are particularly suited for neutron-capture measurements [8]. The total energy detection principle was used by combining the detection system with the so called Pulse Height Weighting Technique (PHWT) [9]. The detectors were placed at 55° with respect to the neutron beam and about at 10 cm distance from the sample under investigation, and facing it (see Figure 3).

In the measurement, a sample of ^{154}Gd ($m=0.263$ g) with well characterized isotopic composition and a natural

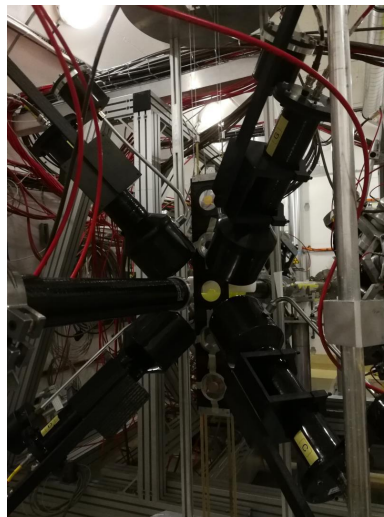


Figure 3. The detection system with the four deuterated scintillation detectors; the sample under investigation and the carbon fiber sample holder are also visible.

Gd sample ($m=8.749$ g) have been used together with samples of ^{197}Au ($m= 1.308$ g), Pb ($m = 6.240$ g) and "empty" ($6 \mu\text{m}$ mylar foil) for the purpose of normalization and background determination. All samples used were cylindrical in shape with 3.0 cm diameter.

3 Data analysis

3.1 Stability, calibrations and assessments

The experimental setup and its performances have been carefully characterized; in particular the detectors response stability, mostly related to the gain of the photomultipliers, has been regularly verified by measurements with standard γ -ray sources, namely the ^{137}Cs , ^{88}Y , Am-Be and Cm-C sources. A gain stability better than 1% was found for all detectors.

Standard γ -ray sources have been also used to obtain reliable amplitude-to-energy calibrations and determine the detectors resolution as a function of the γ -ray deposited energy. Both features are important in the data analysis, because of the modification of the detector response by means of the PHWT. The weighting functions for ^{154}Gd , nat-Gd and Au were obtained by implementing in GEANT4 a software replica of the apparatus and the resolution on the deposited energy. Sample- and background-related weighted counts were used to extract the unnormalized capture yield.

Typically, the saturated resonance method is used to normalize the measured capture yield with the ^{197}Au resonance at 4.9 eV. However, due to a probable misalignment of the gold sample with respect to the neutron beam, the normalization factor obtained in this way was deemed affected by a large uncertainty. In order to circumvent such a problem, resonances related to the $^{155}\text{Gd}(n, \gamma)$ reaction were used for normalization, taking into account its isotopic abundance in the nat-Gd sample, and the declared contamination in the ^{154}Gd one. The resonance parameters re-

cently published in [10] for the $^{155}\text{Gd}(n, \gamma)$ reaction have been used in order to extract the normalization factor (see Figure 4).

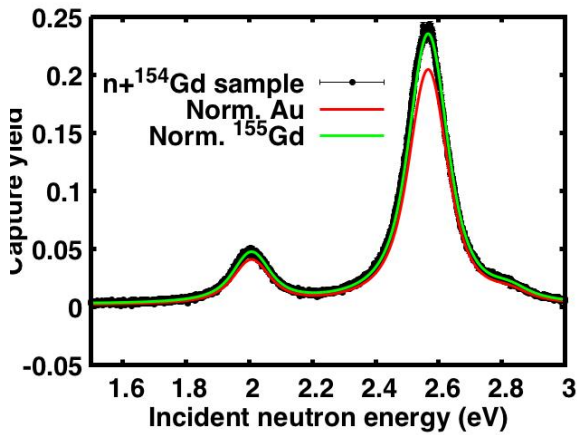


Figure 4. The normalized $^{154}\text{Gd}(n, \gamma)$ capture yield; structures at 2 and 2.5 eV neutron energy are due to the ^{155}Gd presence ($\approx 17.5\%$) in the sample. A discrepancy between gold and ^{155}Gd normalization methods is clearly visible.

The study of the background has been performed by means of dedicated measurements with the aim to evaluate the various components, i.e. the one produced by the neutron beam interaction in the experimental area (without the sample), and the one related to in-beam γ -rays. The first component has been evaluated with the empty-sample, while the in-beam γ -ray background has been obtained by combining data collected with the Pb and the empty-sample. As shown in Figure 5, the main background source arises from the empty-sample counts, that is the beam-related effect not linked to the presence of the sample.

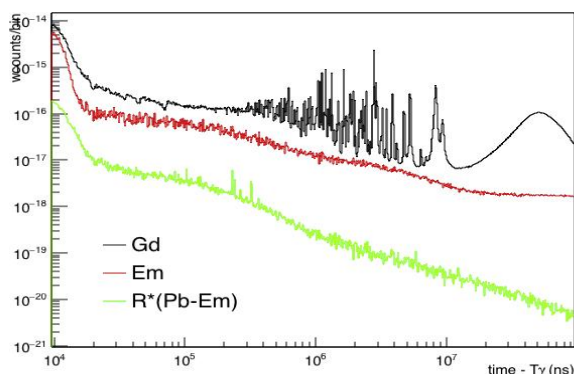


Figure 5. Weighted C_6D_6 time-of-flight spectrum of the ^{154}Gd sample, together with background measurements. The empty-sample spectrum (Em) represents the main background source.

3.2 Resonance Shape Analysis

The Resolved Resonance Region (RRR) is analyzed with the bayesian R-Matrix code SAMMY, using the Reich-Moore approximation. Corrections for experimental conditions such as Doppler broadening, self-shielding and multiple scattering in the sample were taken into account by the code. As starting point, the ENDF/B-VII library resonance parameters were adopted for the fitting procedure. An example of the Resonance Shape Analysis (RSA) is shown in Figure 6, compared to evaluated yield.

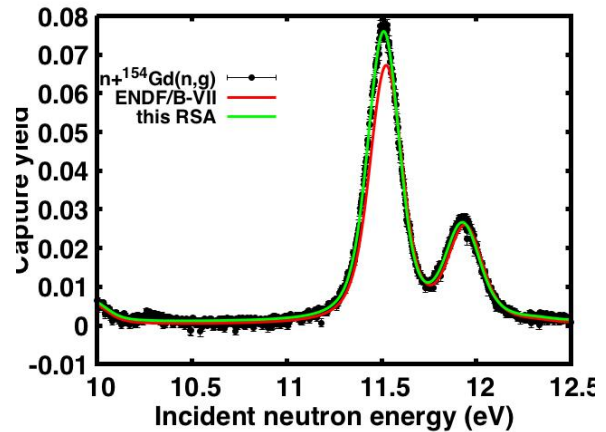


Figure 6. The RSA of the n_{TOF} data performed by SAMMY code compared to ENDF/B-VII evaluations.

A comparison between the capture kernel obtained by the preliminary fitting procedure on the n_{TOF} experimental data and the theoretical one calculated on the basis of the ENDF/B-VII evaluations (see Figure 7), show that on average the n_{TOF} data are $\approx 6\text{-}7\%$ higher than the evaluated data.

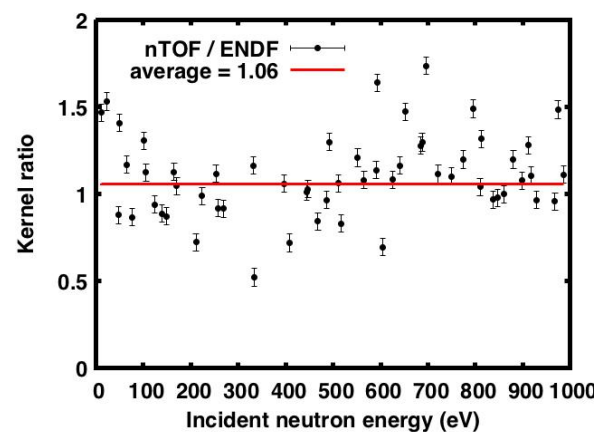


Figure 7. The ratio between the capture kernel obtained by the fit of the n_{TOF} data and the one calculated with the ENDF/B-VII resonance parameters.

3.3 The Unresolved Resonance Region

The reaction rate and consequently the production and the isotopic abundance of ^{154}Gd strongly depends on the

Maxwellian Averaged Cross Section (MACS). Approximately 70-80% of the MACS depends on the Unresolved Resonance Region (URR) and for this reason this represents a particularly important energy region. However, the experimental data available in the literature ([11, 12]) show discrepancies higher than 30% among themselves.

A comparison of the preliminary n_TOF experimental data and ENDF/B evaluation in the same energy region is shown in Figure 8. On average, the n_TOF data are in a quite good agreement with the evaluated data in the URR, although sizable differences are present in some region.

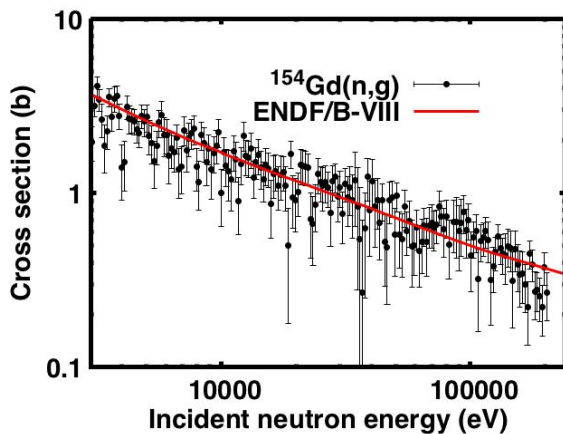


Figure 8. Cross-section of $^{154}\text{Gd}(n, \gamma)$ reaction measured at n_TOF, compared with ENDF/B evaluated data in the URR.

The preliminary results obtained up to now have been used to calculate the ^{154}Gd MACS. We computed a set of AGB models at close-to-solar metallicity with low-to-intermediate stellar masses ($1.5 \leq M/M_{\odot} \leq 3.0$). Based on the preliminary n_TOF data, a general increase of ^{154}Gd (with respect to ^{150}Sm) of about 5% is found. Such an increase is not sufficient to explain the current disagreement between stellar models and observations. We speculate that other neutron capture cross sections in the Sm-Eu-Gd have to be studied in detail as, for instance, the ^{154}Eu neutron capture cross section, for which we do not dispose of an experimental MACS.

4 Conclusions

The results obtained so far in the Resolved Resonance Region and reported in this work have shown a $^{154}\text{Gd}(n, \gamma)$ cross section substantially higher than the evaluated one in the ENDF/B library. Resonance Shape Analysis is still ongoing; new resonance structures up to 2 keV are present in the n_TOF data, which are not reported in any evaluated data library. In the Unresolved Resonance Region, n_TOF data are in a reasonable agreement with the evaluations, thus no big effect is expected on MACS value in this energy region.

Although the results here presented are preliminary and need further confirmation, it can presently be concluded that, based on these new data, no substantial changes in the synthesis of ^{154}Gd have to be expected. As a consequence, the origin of the discrepancy between theory and observations has to be searched in other nuclear ingredients, as the neutron capture cross section on ^{154}Eu , whose decay largely influences the ^{154}Gd abundance.

References

- [1] F. Käppeler *et al.*, *Rev. Mod. Phys.* **83**, 157 (2011)
- [2] N. Prantzos *et al.*, *MNRAS* **476**, 3432 (2018)
- [3] S. Bisterzo *et al.*, *The Astrophysical Journal* **787**, 10 (2014)
- [4] S. Cristallo *et al.*, *The Astrophysical Journal* **801**, 53 (2015)
- [5] K. Lodders *et al.*, *LanB* **4**, 712 (2009)
- [6] M. Barbagallo *et al.*, *Eur. Phys. J. A* (2013) **49**: 156
- [7] P. F. Mastinu *et al.*, CERN-n TOF-PUB-2013-002.
- [8] P. Schillebeeckx *et al.*, *Nucl. Data Sheets*, 113 (2012) 3054.
- [9] A. Borella *et al.*, *Nucl. Instrum. and Methods A*, 577 (2007) 626.
- [10] M. Mastromarco *et al.*, *Eur. Phys. J. A* **55**, 9 (2019)
- [11] K. Wisshak *et al.*, *Phys. Rev. C* **52**, 2762 (1995)
- [12] H. Beer *et al.*, *The Astrophysical Journal* **331**, 1047 (1988)